Compact Electro-Optic Modulators on a Silicon Chip

Michal Lipson, *Member, IEEE*

(Invited Paper)

Abstract—Electro-optic modulators are one of the most critical components in optoelectronic integration, and decreasing their size may enable novel chip architectures not previously possible. Here, we discuss high-confinement resonators as modulators for achieving high performance in micrometer-size structures.

Index Terms—Integrated optics, optical resonators, planar waveguides, silicon-on-insulator technology.

I. INTRODUCTION

THE use of silicon for optical interconnects would enable a platform for a monolithic integration of optics and microelectronics [1]–[4]. Photonics on silicon has been suggested since the 1980s; however, it is only in the last few years, that submicrometer-size photonic structures have been realized. Photonic structures that bend, split, couple, and filter light have recently been demonstrated in silicon [5]–[7], [9]. However, such structures have their flow of light predetermined by the design of the structure and cannot be modified once fabricated. In order to control the flow of light, modulators and switches need to be developed in silicon, where a change in the refractive index induces a change in the transmission properties of the device. One of the main challenges of using silicon as an active photonic material is its low electro-optic coefficient.

The most common electro-optic effects found in compound semiconductors are weak in silicon. Unstrained pure crystalline silicon does not exhibit a linear electro-optic (Pockels) effect. The Franz–Keldysh effect ("electroabsorption") and the Kerr effect (the second-order electro-optic) have very low efficiencies: a refractive index variation of $\Delta n \sim 10^{-5}$ in the near infrared for the Franz–Keldysh effect, and $\Delta n \sim 10^{-8}$ for the Kerr effect for an applied field of 10^5 V/cm. Therefore, high electromagnetic fields potentially close to the breakdown of silicon are required in order to achieve a useful change in the index of refraction.

The most effective mechanism for changing the refractive index in Si at a fast rate is the carrier plasma dispersion effect, which also has the advantage of being polarization independent.

The induced real refractive index and optical absorption coefficient variations (Δn and $\Delta \alpha$, respectively) produced by carrier dispersion at a wavelength of 1.55 μm are given by [10]

$$\Delta n = \Delta n_e + \Delta n_h$$
$$= -[8.8 \times 10^{-22} \Delta N + 8.5 \times 10^{-18} (\Delta P)^{0.8}] \quad (1)$$
$$\Delta \alpha = \Delta \alpha_e + \Delta \alpha_h$$
$$= 8.5 \times 10^{-18} \Delta N + 6.0 \times 10^{-18} \Delta P \quad (2)$$

where Δn_e is the refractive index change due to the electron concentration change, Δn_h is the refractive index change due to the hole concentration change, ΔN (cm^{-3}) is the electron concentration change, ΔP (cm^{-3}) is the hole concentration change, $\Delta \alpha_e$ (cm^{-1}) is the absorption coefficient variations due to ΔN, and $\Delta \alpha_h$ (cm^{-1}) is the absorption coefficient variation due to ΔP. Thus, electrorefractive changes of $\Delta n \sim 2 \times 10^{-3}$ at a wavelength of 1.55 μm can be produced with a depletion or injection of 10^{18} carriers/cm^3.

Recently, several structures in silicon have been demonstrated [11]–[17] using the plasma dispersion effect for modulation. However, such structures are large with dimensions of the order of millimeters. The fact that the electro-optical properties of silicon are weak allowed the use of such dimensions with a small change in the index of refraction of silicon, resulting in a correspondingly small modulation of the transmission of the necessarily large device. Liu *et al.* [11], for example, have recently demonstrated a high-speed silicon optical modulator based on a metal-oxide-semiconductor (MOS) configuration. The work was the first one to show a high-speed optical active device on silicon—a critical milestone towards the optoelectronic integration on silicon. Liao *et al.* [17] have also recently presented a modulator capable of 10 Gb/s. However, due to the weak dependence of silicon's index of refraction on the electron–hole pair concentration, and the limited mode confinement in the active region of the MOS device, the devices in [11] have relatively large lengths of the order of millimeters.

The use of resonators enables high modulation in silicon using compact devices. The transmission of a resonator is given approximately by

$$T = \frac{T_{\max}}{1 + \left(\frac{4nL}{\pi \Delta \lambda}\right)^2 \sin^2 \left(\frac{2\pi}{\lambda} nL\right)} \quad (3)$$

where λ is the wavelength incident on the resonator, and $\Delta \lambda$ is the full-width at half maximum of the transmission at resonance, determined by the quality of the resonator and its geometrical configuration. The ability of a resonator to circulate light within the cavity at the resonance wavelength can be used to increase the optical path length without increasing the physical device length unlike, for example, a Mach–Zehnder device. After a

typical photon lifetime in the resonator given by $\tau_{ph} = \lambda L/\lambda c$, light exits the device with transmitivity $T = T_{max}$. At all other wavelengths within the stop band, light destructively interferes in the cavity region and is not transmitted through the resonator (it is either reflected or directed to a different path, depending on the geometrical configuration of the modulator). Note that for waveguide resonators, typically micrometer in size with $\lambda/\Delta\lambda \sim 10^2 - 10^4$, the photon lifetime is typically short, of the order of a few picoseconds. This is important in order to guarantee fast operation of the resonator as a modulator. In order to achieve modulation using resonators, the resonances of the device are tuned by modifying the index of refraction of the structure. Due to the strong light confinement nature of the device, a small change in index of refraction induces a strong tuning of the resonance. From (3), one can note that if the refractive index is changed by a small amount, the transmission can change significantly at or near resonance, resulting in a strong-intensity modulation of the signal transmitted through the resonator.

In [18], a ring resonator is used as a modulator for achieving high modulation in micrometer-size structures. For a ring resonator, we show that an index change as small as 10^{-3} is sufficient to tune the resonance by 1 nm and modulate the output intensity of the device by nearly 100%. This index change is achieved by carrier injection. Note that the disadvantage of using resonators for modulation versus Mach–Zender, for example, is the high temperature sensitivity of the device. For example, from (3), for a resonator with $\lambda/\Delta\lambda \sim 10^3$, a silicon thermo-optic effect of 2×10^{-4}/degree induces a modulation of approximately 5% in the transmission for every degree change. In order to minimize the effect of the temperature variations on the index of refraction, recent studies have been investigating the use of strain in the waveguide structure between the silicon and the oxide cladding, created by using a variety of oxidation methods for compensating the effects of temperature variations on the index of refraction [19], [20].

II. ELECTRO-OPTIC MODULATION IN SILICON RING RESONATORS

The carrier concentration in silicon can be varied by injection, accumulation, depletion, or inversion of carriers. The p-i-n diodes [21], [22] and metal-oxide-semiconductor field-effect-transistors (MOSFET) [23], [24] may be employed for this purpose. In MOS devices, the carriers are typically located only in a small region, resulting in a small overlap between the optical mode and the nonequilibrium charge distribution in the waveguide, and thereby leading to a smaller effective index variation in a MOS system than that in a p-i-n configuration [23]. A small effective index change requires a very long structure, of the order of millimeters, in order to induce a significant modulation depth (see (5), [24]). For this reason, we choose to work with p-i-n devices. Fig. 1 (inset) shows a schematic cross section of a ridge waveguide with an integrated lateral p-i-n diode for electro-optic modulation [22]. It consists of a ridge waveguide with a p^+ region and an n^+ region defined in the slab at each side of the ridge. The waveguide is fabricated on a silicon-on-insulator (SOI) wafer comprising of three layers, one single-crystal layer
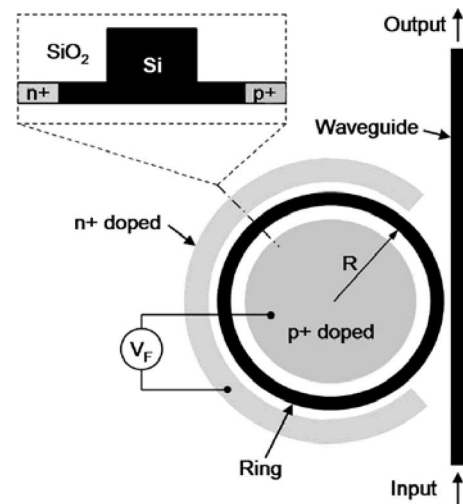

Fig. 1. Schematic layout of the ring-resonator-based modulator. The inset shows the schematic of the cross section of the ring (from [37]).
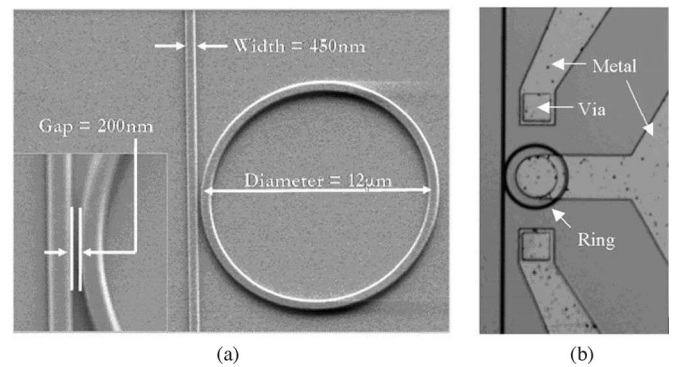

Fig. 2. SEM and microscopic images of the electro-optic device. (a) Top-view SEM image of the ring coupled to the waveguide with a zoom-in picture of the coupling region. (b) Top-view microscopic image of the ring resonator after the metal contacts are formed (from [37]).

of silicon, a base silicon substrate, and a thin insulator (BOX) that acts as bottom cladding and therefore prevents light leakage to the substrate. The silicon layer (device layer) has an n-type background doping concentration of 10^{15} cm^{-3}, whereas a uniform doping concentration of $\sim 10^{19}$ cm^{-3} for both p^+ and n^+ regions is considered. A top SiO$_2$ cladding layer covers the whole structure. Using configurations with a cross section similar to the one shown in Fig. 1 in waveguides and interferometers, several devices have been demonstrated [24]–[35]. In [36], the authors embedded a p-i-n in a large rib waveguide and demonstrated a 20-MHz modulator. The speed of this device is limited by the free-carrier recombination time in the waveguide. By embedding the ridge waveguide into a ring resonator with $Q = 40\,000$ (as the one shown in Fig. 1), we demonstrated in [22] and [37] the modulation depth of 15 dB with a modulation speed of 1.5 Gb/s.[1] The high modulation speed was achieved using both forward and reverse bias for injecting and extracting carriers, respectively.

---

[1]Since the submission of the paper, we have demonstrated modulation speeds of 12.5 Gb/s using a similar device to the one shown in Fig. 1. These results are reported in [38].
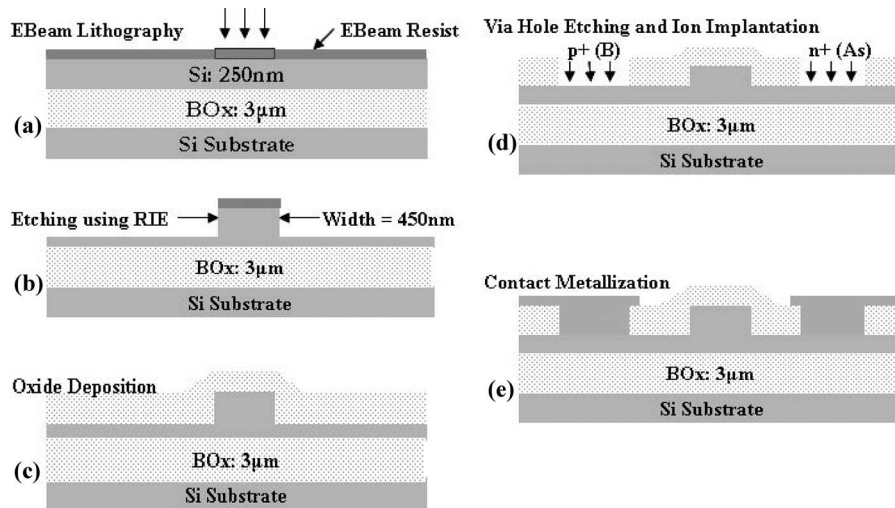
Fig. 3. Fabrication process flow. (a) EBeam lithography on the SOI wafer coated with photoresist to define the waveguides and rings. (b) RIE etching. (c) Deposition of oxide. (d) Etching of holes and ion implantation. (e) Contact metallization.
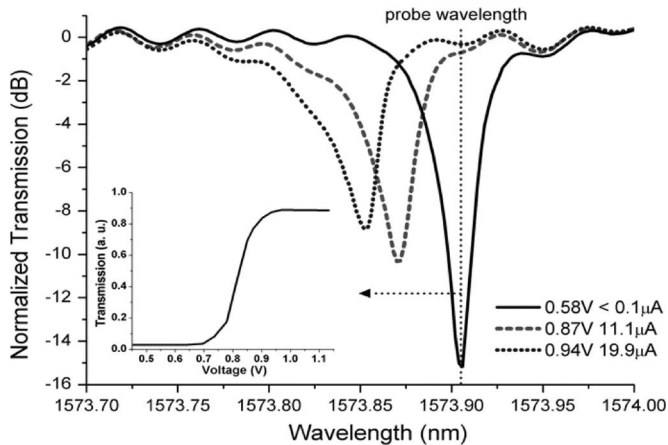

Fig. 4. DC measurements of the ring resonator. The main panel shows the transmission spectra of the ring resonator at the bias voltages of 0.58, 0.87, and 0.94 V, respectively. The inset shows the transfer function of the modulator for light with wavelength of 1573.9 nm (from [37]).

Fig. 2 shows the SEM of an electro-optic modulator device [37] based on the ring resonant light-confining structure. The structures in [37] were patterned by electron-beam lithography and subsequently etched by inductively coupled, plasma reactive ion etching on Smart Cut SOI wafers with a buried 3-μm-thick oxide layer. These required dimensions can, in principle, be achieved by more cost-effective methods such as current production photolithography. The fabrication process flow for the structures is described in Fig. 3.

The relative TE-like transmission through the modulator around the resonance of 1574 nm at different bias of the p-i-n junction is shown in Fig. 4. The transmission was measured using a signal coupled into the silicon waveguide by an external tapered-lensed fiber and an on-chip fiber-to-waveguide nanotaper coupler [39]. The fiber-waveguide coupling losses are measured to be approximately 2 dB. The solid curve shows the spectrum when the forward bias (0.59 V) on the p-i-n junction is much lower than the built-in potential of the junction, and

the current through the junction is below the detection limit (0.1 μA). The spectrum shows a 15-dB drop of transmission at the resonant wavelength of 1574.9 nm. The low transmission at this wavelength is the initial condition of a "dark-to-light" intensity modulator. The 3-dB bandwidth of the resonance $\Delta\lambda$ is 0.04 nm measured from the spectrum, corresponding to a quality factor of 39350, defined as $Q = \lambda/\Delta\lambda$. This Q factor corresponds to a cavity photon lifetime of $\tau_{\mathrm{cav}} = \lambda^2/(2\pi c\, \Delta\lambda_{\mathrm{FWHM1}}) = 33$ ps, where c is the speed of light in vacuum. Thus, despite the resonant nature of the structure, the photon confinement of the modulator does not limit its speed. The small ripples ($\sim$1 dB) on the waveform originate from the reflections at both ends of the waveguide, which can be eliminated by the antireflection coating. The electron–hole pair density in the cavity increases as the forward bias on the p-i-n junction increases. The dashed and dotted curves in Fig. 3 show the spectra, when the bias voltage is 0.87 and 0.94 V, and the current is 11.1 and 19.9 μA, respectively. In both cases, the resonance is blue-shifted due to the lowering of the effective index caused by the increase of electron–hole pair density in the cavity [10]. The depths of the notches in the spectra decrease due to the increased absorption loss in the ring induced by the electrons and holes. The extra absorption per round trip in the ring is estimated from the spectra as 0.02 dB at 0.87-V bias and 0.04 dB at 0.94-V bias. At the probe wavelength of 1573.9 nm, one can note from Fig. 4 that 97% (15 dB) modulation can be obtained with less than 0.3-V bias voltage change. At this wavelength, since light does not couple to the ring when the electrons and holes are generated, the effect of the extra absorption in the ring on the modulation is less than 0.1 dB.

The light confining nature of the modulator not only enables the shrinking of the device size, but also enables a high-speed operation under the p-i-n configuration. The p-i-n configuration of the modulator, as opposed to the MOS configuration [11], is important for achieving high modulation depth, since the overlap between the region where the index is changed and the optical mode of the waveguide is large. However, the p-i-n
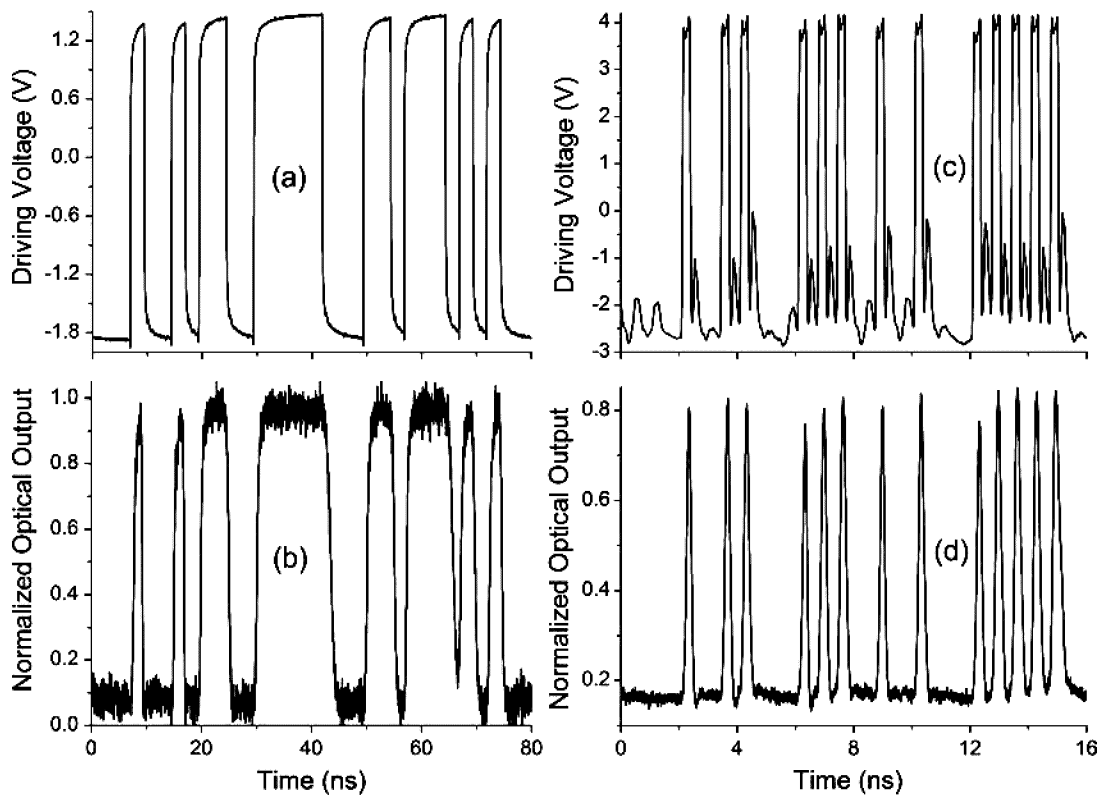
Fig. 5. Waveforms of the electrical driving signal and the transmitted optical signal. (a) Waveform of the 32-bit pseudorandom NRZ signal at 0.4 Gb/s applied on the modulator. (b) Waveform of the output optical power of the modulator with NRZ modulation, normalized to the output power when the ring resonator is completely out of resonance. (c) Waveform of the $2^7 - 1$ pseudorandom bit sequence RZ signal at 1.5 Gb/s applied on the modulator. (d) Waveform of the normalized output optical power of the modulator with RZ modulation (from [37]).

devices have been traditionally considered as relatively slow devices when compared to the MOS devices. In p-i-n devices, while the extraction of electrons and holes in reverse-biased operation can be fast, down to tens of picoseconds [40], the injection of electrons and holes in forward-bias operation is slow, which limits the rise time of the p-i-n to be of the order of 10 ns, as measured in our device. The resonating nature of the modulator removes this speed limitation. The inset of Fig. 3 shows the transfer function of the device, i.e., the transmission of the modulator at the wavelength of 1573.9 nm with different bias voltages. This transfer function shows that the resonating nature of the device enables voltages larger than 0.9 V to be applied without modifying the transmission response ($T \sim 1$). This is because, at these voltages, the resonance of the device is completely detuned from the probe wavelength. This insensitivity of the optical transmission at higher bias voltage is in strong contrast to Mach–Zehnder modulators, in which higher voltage strongly affects the transmission. When the device is operating at higher voltages, the optical transmission can go to ~ 1 well before the p-i-n junction reaches its steady state. This means that the RC time determining the electrical rise time (of the order of 10 ns) does not limit the speed of the device. The optical transmission rise time in a resonator is much shorter (of the order of 80 ps) and does not follow the electrical rise time, which is critical for achieving high-speed smodulation.

In order to measure the dynamic response of the modulator, electrical signals generated by a pulse-pattern generator and a wideband microwave amplifier are used to drive a modulator. The output of the waveguide is sent to a 12-GHz detector, and the waveform is recorded on an oscilloscope. Fig. 5(a) and (b) shows the waveform of the driving signal using both the nonreturn-to-zero (NRZ) pattern and the optical output, demonstrating high modulation depths at 0.4 Gb/s. The peak-to-peak voltage (Vpp) of the driving signal is 3.3 V, from -1.85 to $+1.45$ V. The speed of the device is limited by the fact that the p-i-n junction is formed on only one part of the ring resonator (see Fig. 1). During the forward-biasing period, the electrons and holes diffuse into the section of the ring that is not a part of the p-i-n junction (the section close to the straight waveguide), where they cannot be efficiently extracted during the reverse-biased period, leading to a longer fall time (~ 1.5 ns) following consecutive "1"s. This longer fall time is determined by the intrinsic surface recombination electrons and holes lifetime in the non-p-i-n region, which is of the order of ~ 1 ns, and is independent of the reverse-biased voltage. This can be clearly seen following a longer injection time, for example, in Fig. 5(b) around 40 and 60 ns, where the signal following the longer forward bias has a longer decay time. In order to verify this point we used a return-to-zero (RZ) pattern, where the injection time is short, minimizing the effect of carrier diffusion. Using

this pattern, we have been able to demonstrate the data rate of 1.5 Gb/s [see Figs. 5(c) and 1(d)].[1]

III. Dynamics Controlling the Speed of the Modulator

The speed of the device is limited by: 1) the photon lifetime within the resonating structure; 2) the carrier injection time; and 3) the carrier extraction time.

The photon lifetime depends on the geometry of the resonating structure, and for a typical resonator dimensions of about 10 μm with $Q \sim 10^4$, it is of the order of picoseconds. This lifetime, therefore, should not limit the speed of the modulator.

The injection and extraction times are limited by the combined optical and electrical characteristics of the devices. We [37] have shown that it is possible to operate the device in a nonsteady state regime in order to achieve much higher speeds than the traditional carrier injection devices, by controlling the dynamics of the modulator. In [37], the device was operated in an overdrive mode. In this mode, the voltage (positive and negative), much larger than the one needed in order to induce enough index change to modulate the device, is applied on the device for only a short time, much shorter than the equilibrium time of the junction. When operating as an "on–off" modulator, the ring resonator is "on" resonance when there are no charge carriers within the ring resonator, and the modulator is in "off" state when there are carriers within the resonator and the transmission is minimal. When the junction is forward biased, the steady-state carrier density is proportional to the current. A 10-μA current flowing through the diode is sufficient to detune the resonance and turn the modulator on [37]. The junction reaches its steady-state carrier density after about 10 ns. Stronger forward biasing of the diode, which corresponds to a higher steady-state carrier density, allows the modulator to be turned on well before the junction reaches its steady state. For example, the optical rise time will be reduced 200 times to 50 ps, if the steady-state current is 2 mA. When the p-i-n junction is reverse biased, the carriers are swept out of the junction by the electric field. The fall time of the modulator is therefore determined by the length of the junction and the voltage applied. Assuming that a 2-V potential is dropped over a 1-μm long junction, the switch time is limited by the saturated speed of the hole movement with $v_d \sim 5 \times 10^{-6}$ cm/s. Therefore, the fall time is ultimately limited by the time required for the carriers to move out of the micrometer waveguide.

In order to estimate the fundamental limitations for the carrier injection time, we consider the carrier density required to detune the resonance

$$\frac{n_{\text{eff}}}{\Gamma \alpha_f Q}$$

where Γ is the mode confinement factor, Q is the quality factor of the resonator, n_{eff} is the effective index of the optical mode, and $\alpha_f \approx 1.35 \times 10^{-21}$ cm^3 is the coefficient of free-carrier dispersion effect. In order to reduce the optical rise time N times, the steady-state carrier density needs to be N times the required value for turning the modulator on. The carrier extraction
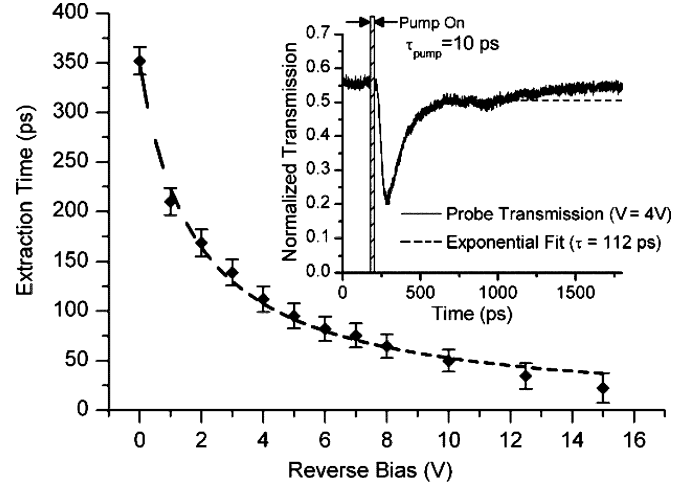

Fig. 6. Carrier extraction time as a function of reverse-bias voltage. The inset shows the temporal probe signal for reverse-bias $V = 4$ V and the exponential fit used to obtain the extraction time (1/e point) (from [40]).

speed is limited by the contact resistance and is given by

$$\frac{V}{qR}$$

where R is the contact resistance, V is the reverse-bias voltage, and $q = 1.6 \times 10^{-19}$C. Therefore, for the electro-optic modulator in [18], given $\Gamma \sim 0.8, R \sim 10\,\Omega, V = 2$ V, and $V_I \approx 5 \times 10^{-12}$ cm^3 for a 12-μm-diameter ring, $Q \sim 4 \times 10^4, n_{\text{eff}} \approx 2.5$, the fall time is limited by

$$t_{\text{fall}} \approx \frac{qR}{V} N \frac{n_{\text{eff}}}{\Gamma \alpha_f} \frac{V_I}{Q} \approx 50 \text{ ps}.$$

For a $\sim$3-V voltage swing, we can expect the modulator to give $\sim$50-ps rise and fall time, and at least 10-Gb/s modulation speed. This speed can be easily increased to values greater than 10 Gb/s by increasing the Q factor of the device and decreasing the contact resistance. Conservative changes in certain parameters in the above equation, such as an increase of Q by a factor of 2 and a decrease of the contact resistance also by a factor of 2, reduces t_{fall} to a value of 10 ps, which corresponds to a modulation speed of 40 Gb/s.

In order to experimentally evaluate the carrier extraction time of the device in [37], the device was optically modulated. A beam of light was used to photoexcite the charge carriers, while a second beam acted as a probe signal. Using the diode in reverse bias, we experimentally found that the extraction time can be brought down to 50 ps. Fig. 6 shows the measured extraction time taken from [41]. The inset of Fig. 6 shows the probe signal for a reverse-bias voltage of 4 V. As seen, the probe signal initially decreases after the pump pulse is applied. The time it takes for this transition to occur is determined by the resonant cavity lifetime τ_{probe}, which dictates how quickly the optical field in the resonator is built up. The initial decrease is then followed by an exponential increase, corresponding to the extraction time of the photoexcited carriers as determined by fitting a simple exponential decay to this part of the probe signal temporal response (shown as a dashed line over the temporal signal). After the
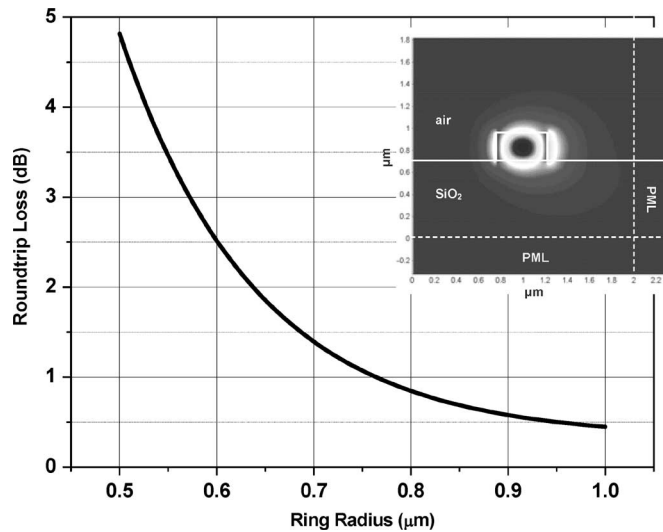
Fig. 7.   Roundtrip losses in a ring resonator as a function of ring radius. Mode of a waveguide bend found by our mode-solver (inset) (from [41]).

exponential increase, the probe signal does not return to its initial state, but instead slowly increases, as the fraction of the carriers generated in the ring is not extracted by the diode, because it encompasses only two-thirds of the ring. The dynamics of any carrier in the remaining part of the ring is solely determined by slow recombination mechanisms, and is thus equivalent to the open-circuit recombination time of 1.19 ns. If the diode was to encompass the entire ring, then the carrier dynamics would solely be determined by the reverse-biased diode carrier extraction time. Note also that a high voltage was necessary in order to achieve a 50-ps extraction time. This high modulation depth is needed mainly due to the high resistance of the device and could be improved by at least an order of magnitude.

In order to experimentally evaluate the carrier injection time of the device in [37], we measured the modulator response at high voltages (8 Vpp), at a single frequency of 5.5 GHz. We find a rise time (injection time) of 88 ps. A higher voltage is needed to increase the speed of the device. The high voltage of 8 Vpp was necessary due to the high contact resistance of the present device. The short rise time indicates that the device is capable of operating at data rates higher than 10 Gb/s in short interconnection systems, where the modulator is the bottleneck of the transmission speed.[1]

IV. MINIMIZATION OF THE SIZE OF THE RESONATORS

The speed of the device could be improved with the minimization of the size of the device. The limiting factor in shrinking the size of resonators is the radiation loss. This loss can be evaluated numerically. The optical field distribution is shown in the inset of Fig. 7. The simulated silicon waveguide measures 450 by 250 nm, is surrounded by SiO_2 at the bottom and air at the top and sides, and has a 1-μm bending radius.

Fig. 7 shows the roundtrip losses in a silicon ring resonator as a function of the ring radius [42]. From the figure, an optical field propagating in a ring of radius 1 μm suffers losses of less than 0.5 dB. We expect these losses to have an insignificant ef-

fect on the performance of the device, since they are much lower than the current measured propagation losses of approximately 10 dB/cm in tight bends. Note that these losses are much higher than the measured losses in straight high confinement waveguides (typically 3 dB/cm) [9] due to the high overlap of the field with the roughness fluctuations in the sidewall of the waveguide (inset of Fig. 7).

V. CONCLUSION

The ring resonator is a promising approach for enabling high speed modulation in micrometer-size device on silicon. A high modulation p-i-n junction embedded in the ring resonator is used, in which the modulation of the index strongly affects the transmission properties. We show that despite the carrier injection nature of the device, the speed of modulation is not limited by the carrier lifetime. Instead, it is limited by the photon lifetime, carrier injection, and carrier extraction time. We show that the device is capable of operating at data rates higher than 10 Gb/s in short interconnection systems, where the modulator is the bottleneck of the transmission speed. Such ring resonators could be further shrunk in size down to 1 μm in bending radius without suffering high radiation losses, enabling further increase in data rates.

ACKNOWLEDGMENT

REFERENCES

[1] R. C. Johnson. (2002, Feb. 28). Intel reveals long-term goals for silicon photonics sensors. *Electron. Eng. Times* [Online]. Available: http://www.eetimes.com/semi/news/OEG20020228S0033
[2] L. C. Kimerling, "Photons to the rescue: Microelectronics becomes microphotonics," *Electrochem. Soc. Interface, Summer 2000*, vol. 9, no. 2, pp. 28–32.
[3] C. Gunn, "CMOs photonics—SOI learns a new trick," in *Proc. IEEE 2005 Int. Silicon on Insulator (SOI) Conf.* Oct. 3–6, 2005, pp. 7–13.
[4] B. Jalali, S. Yegnanarayanan, T. Yoon, T. Yoshimoto, I. Rendina, and F. Coppinger, "Advances in silicon-on-insulator optoelectronics," *IEEE J. Sel. Topics Quantum Electron.*, vol. 4, no. 6, pp. 938–947, Nov./Dec. 1998.
[5] V. R. Almeida, R. Panepucci, and M. Lipson, "Compact mode conversion for highly-confined waveguides," in *Proc. Integr. Photon. Res. (IPR) Conf.*, Washington, DC, 2003, pp. 230–233.
[6] B. Jalali, "Silicon photonics," *Proc. SPIE*, vol. 3290, pp. 238–45, 1997.
[7] K. K. Lee, "Transmission and routing of optical signals in on-chip waveguides for silicon microphotonics," Ph.D. dissertation, Massachusetts Inst. Technol., Cambridge, MA, 2001.
[8] M. Salib, M. Morse, L. Liao, R. Jones, D. Samara-Rubio, A. Liu, A. Alduino, and M. Paniccia, "Silicon photonics," *Intel Technol. J.*, vol. 8, no. 2, pp. 143–160, 2004.
[9] Y. A. Vlasov and S. J. McNab, "Losses in single-mode silicon-on-insulator strip waveguides and bends," *Opt. Express*, vol. 12, no. 8, pp. 1622–1631, 2004.
[10] R. A. Soref and B. R. Bennett, "Kramers–Kronig analysis of electro-optical switching in silicon," *Proc. SPIE*, vol. 704, pp. 32–37, 1987.
[11] A. Liu, R. Johnes, L. Liao, D. Samara-Rubio, D. Rubin, O. Chohen, R. Nicolaescu, and M. Paniccia, "A high-speed silicon optical modulation based on a metal-oxide-semiconductor capacitor," *Nature*, vol. 427, pp. 615–618, 2004.
[12] T. Sadagopan, S. J. Choi, S. J. Choi, P. D. Dapkus, and A. Bond, "High-speed, low-voltage modulation in circular WGM microresonators," presented at the IEEE LEOS Summer Top. Meeting, San Diego, CA, Jun. 28–30, 2004.

[13] P. Dainesi, A. Kung, M. Chabloz, A. Lagos, P. Fluckiger, A. Ionescu, P. Fazan, M. Declerq, P. Renaud, and P. Robert, "CMOS compatible fully integrated Mach–Zehnder interferometer in SOI technology," *IEEE Photon. Technol. Lett.*, vol. 12, no. 6, pp. 660–662, Jun. 2000.

[14] C. K. Tang and G. T. Reed, "Highly efficient optical phase modulator in SOI waveguides," *Electron. Lett.*, vol. 31, no. 6, pp. 451–452, 1995.

[15] A. Cutolo, M. Iodice, P. Spirito, and L. Zeni, "Silicon electro-optic modulator based on a three terminal device integrated in a low-loss single-mode SOI waveguide," *J. Lightw. Technol.*, vol. 15, no. 3, pp. 505–518, Mar. 1997.

[16] A. Sciuto, S. Libertino, A. Alessandria, S. Coffa, and G. Coppola, "Design, fabrication, and testing of an integrated Si-based light modulator," *J. Lightw. Technol.*, vol. 21, no. 1, pp. 228–235, Jan. 2003.

[17] L. Liao, D. Samara-Rubio, M. Morse, A. Liu, D. Hodge, D. Rubin, U. D. Keil, and T. Franck, "High speed silicon Mach–Zehnder modulator," *Opt. Express*, vol. 13, no. 8, pp. 3129–3135, Apr. 2005.

[18] V. R. Almeida, C. A. Barrios, R. R. Panepucci, and M. Lipson, "All-optical control of light on a silicon chip," *Nature*, vol. 431, no. 7012, pp. 1081–1084, 2004.

[19] P. Cheben, D. -X. Xu, S. Janz, and A. Delage, "Scaling down photonic waveguide devices on the SOI platform," *Proc. SPIE*, vol. 5117, pp. 147–156, 2003.

[20] S. M. Weiss, M. Molinari, and P. M. Fauchet, "Temperature stability for silicon-based photonic band-gap structures," *Appl. Phys. Lett.*, vol. 83, no. 10, pp. 1980–1982, 2003.

[21] C. Z. Zhao, E. K. Liu, G. Z. Li, Y. Gao, and C. S. Guo, "Zero-gap directional coupler switch integrated into a silicon-on-insulator for 1.3-μm operation," *Opt. Lett.*, vol. 21, no. 20, p. 1664, 1996.

[22] C. A. Barrios, V. R. Almeida, and M. Lipson, "Electro-optic modulation of silicon-on-insulator submicrometer-size waveguide devices," *J. Lightw. Technol.*, vol. 21, no. 10, pp. 2332–2339, Oct. 2003.

[23] S. R. Giguere, L. Friedman, R. A. Soref, and J. P. Lorenzo, "Simulation studies of silicon electro-optic waveguide devices," *J. Appl. Phys.*, vol. 68, pp. 4964–4970, 1990.

[24] G. Cocorullo, M. Iodice, and I. Rendina, "All-silicon Fabry–Perot modulator based on the thermo-optic effect," *Opt. Lett.*, vol. 19, no. 6, p. 420, 1994.

[25] X. Xiao, J. C. Sturm, K. K. Goel, and P. V. Schwartz, "Fabry–Perot optical intensity modulator at 1.3 μm in silicon," *IEEE Photon. Technol. Lett.*, vol. 3, no. 3, pp. 230–231, Mar. 1991.

[26] Y. L. Liu, E. K. Liu, S. L. Zhang, G. Z. Li, and J. S. Luo, "Silicon 1 × 2 digital optical switch using plasma dispersion," *Electron. Lett.*, vol. 30, no. 2, p. 130, 1994.

[27] Y. Liu, E. Liu, G. Li, S. Zhang, J. Luo, F. Zhou, M. Cheng, B. Li, and H. Ge, "Novel silicon waveguide switch based on total internal reflection," *Appl. Phys. Lett.*, vol. 64, pp. 2079–2080, 1994.

[28] C. Z. Zhao, G. Z. Li, E. K. Liu, Y. Gao, and X. D. Liu, "Silicon on insulator Mach–Zehnder waveguide interferometers operating at 1.3 μm," *Appl. Phys. Lett.*, vol. 67, pp. 2448–2449, 1995.

[29] M. Y. Liu and S. Chou, "High-modulation-depth and short-cavity-length silicon Fabry–Perot modulator with two grating Bragg reflectors," *Appl. Phys. Lett.*, vol. 68, pp. 170–172, 1995.

[30] C. Z. Zhao, E. K. Liu, G. Z. Li, Y. Gao, and C. S. Guo, "Zero-gap directional coupler switch integrated into a silicon-on-insulator for 1.3-μm operation," *Opt. Lett.*, vol. 21, no. 20, p. 1664, 1996.

[31] A. Cutolo, M. Iodice, A. Irace, P. Spirito, and L. Zeni, "An electrically controlled Bragg reflector integrated in a rib silicon on insulator waveguide," *Appl. Phys. Lett.*, vol. 71, pp. 199–201, 1997.

[32] ——, "Silicon electro-optic modulator based on a three terminal device integrated in a low-loss single-mode SOI waveguide," *J. Lightw. Technol.*, vol. 15, no. 3, pp. 505–518, Mar. 1997.

[33] C. Z. Zhao, A. H. Chen, E. K. Liu, and G. Z. Li, "Silicon-on-insulator asymmetric optical switch based on total internal reflection," *IEEE Photon. Technol. Lett.*, vol. 9, no. 8, pp. 1113–1115, Aug. 1997.

[34] G. Coppola, A. Irace, M. Iodice, and A. Cutolo, "Simulation and analysis of a high-efficiency silicon optoelectronic modulator based on a Bragg mirror," *Opt. Eng.*, vol. 40, pp. 1076–1081, 2001.

[35] A. Sciuto, S. Libertino, A. Alessandria, S. Coffa, and G. Coppola, "Design, fabrication, and testing of an integrated Si-based light modulator," *J. Lightw. Technol.*, vol. 21, no. 1, pp. 228–235, Jan. 2003.

[36] C. K. Tang and G. T. Reed, "Highly efficient optical phase modulator in SOI waveguides," *Electron. Lett.*, vol. 31, pp. 451–452, 1995.

[37] Q. Xu, B. Schmidt, and M. Lipson, "Micrometer-scale silicon electro-optic modulator," *Nature*, vol. 435, no. 7040, pp. 325–327, 2005.

[38] Q. Xu, B. Schmidt, J. Shakya, S. Manipatruni, and M. Lipson, "WDM silicon modulators based on micro-ring resonators," presented at the IEEE Lasers Electro-Opt. Soc. Annu. Meeting, Montreal, QC, Canada, Oct. 29–Nov. 2, 2006.

[39] V. R. Almeida, R. R. Panepucci, and M. Lipson, "Nanotaper for compact mode conversion," *Opt. Lett.*, vol. 28, pp. 1302–1304, 2003.

[40] J. Muller, "Thin silicon film p-i-n photodiodes with internal reflection," *IEEE Trans. Electron. Devices*, vol. ED-25, no. 2, pp. 247–253, Feb. 1978.

[41] S. F. Preble, Q. Xu, B. S. Schmidt, and M. Lipson, "Ultrafast all-optical modulation on a silicon chip," *Opt. Lett.*, vol. 30, no. 21, pp. 2891–2893, 2005.

[42] C. Manolatou and M. Lipson, "All-optical silicon modulators based on carrier injection by two-photon absorption," *J. Lightw. Technol.*, vol. 24, no. 3, pp. 1433–1439, Mar. 2006.

Michal Lipson (M'02) received the B.S., M.S., and Ph.D. degrees in physics from the Technion—Israel Institute of Technology, Haifa, Israel in 1992, 1994, and 1998, respectively.

In December 1998, she joined the Department of Material Science and Engineering at Massachusetts Institute of Technology (MIT), Cambridge, as a Postdoctoral Associate. In 2001, she joined the Department of Electrical and Computer Engineering at Cornell University, Ithaca, NY, as an Assistant Professor. Her current research interests include novel on-chip nanophotonics devices.

Dr. Lipson was the recipient of a National Science Foundation CAREER Award in 2004 and the IBM Faculty Award in 2006. She is currently a Topical Editor of *Optics Letters*.